2.32-2.78 (4 H, ABCM, 7-$CH_2CH_2CO_2$), 3.01 (2 H, t, 6b), 3.24, 3.40, 3.41 (3 H each, s, ring Me), 3.50 (3 H, s, 7-$CCCO_2Me$), 3.65 (3 H, s, 6-$CCCO_2Me$), 3.97 (2 H, t, 6a), 5.99, 6.07, 6.11, 6.24 (1 H, each, dd, vinyl), 7.98 (2 H, m, vinyl), 8.82, 8.91 (1 H each, s, meso γ, δ), 9.62, 9.71 (1 H each, s, meso α, β), -2.45 ppm (2 H, br s, NH); UV-vis λ_{max} (ϵ_M) 651 nm (41 000), 597 (8000), 533 (8600), 501 (15 800), 402 (159 000).

Acknowledgment. We thank Dr. Russell Timkovich who performed the HPLC analysis verifying the synthetic lactochlorin. We also thank Dr. K. Hallenga and the Michigan Molecular Institute for the use of the 360-MHz NMR to obtain an NOE measurement. This work was supported by the National Institutes of Health (Grant GM 34468), which funds our continued collaboration with Thomas Loehr and Laura Andersson at OGC. C.S. acknowledges the support of a SOHIO Fellowship.

Multicomponent Redox Catalysts for Reduction of Large Biological Molecules Using Molecular Hydrogen as the Reductant

Shuchi Chao, Richard A. Simon, Thomas E. Mallouk, and Mark S. Wrighton*

Contribution from the Department of Chemistry, Massachusetts Institute of Technology, Cambridge, Massachusetts 02139. *Received June 22, 1987*

Abstract: One-electron reduction of the large biological molecules horse heart cytochrome *c*, sperm whale myoglobin, and horseradish peroxidase using H_2 as the reductant can be catalyzed by two-component, high surface area heterogeneous catalysts. The catalysts can be prepared by first functionalizing high surface area SiO_2 with a polycationic polymer into which is dispersed MCl_4^{2-} (M = Pd, Pt). Reduction with H_2 yields elemental Pd or Pt dispersed in the polymer. The particles are finally functionalized with a redox polymer derived from hydrolysis of $Si(OR)_3$ groups of an *N,N'*-dialkyl-4,4'-bipyridinium- or from a cobalticenium-based monomer. The two components of the heterogeneous catalysts are the buried noble metal capable of activating the H_2 and the redox polymer, which can equilibrate both with the noble metal and with the large biological molecule. Reduction of the large biological molecules in aqueous solution can be effected at room temperature and 1 atm H_2 using the catalysts under conditions where the biological materials would not be reducible with H_2 alone or when the noble metal alone would be used as the catalyst.

In this article we report the synthesis and characterization of two-component, high surface area catalysts for the reduction of certain biological redox molecules using H_2 as the reductant (Scheme I). The catalysts that have been synthesized have a component, Pd or Pt, for the activation of the H_2 that is interfaced with a second component, a redox mediator, that is a one-electron, outer-sphere type redox reagent that is reducible with the H_2 and can in turn reduce the biological redox reagent. The basic idea involved is to convert the inert, two-electron, reductant H_2 to two, reactive, one-electron, surface-confined, outer-sphere reducing equivalents. The need to use the one-electron, outer-sphere reducing reagents stems from the general finding that large biological molecules do not interface well with the surfaces of conductors,[1-3] particularly when contaminated with biological impurities.

Scheme I. Catalyst Particle for Reduction of Biological Redox Molecule Using H_2 as the Reductant

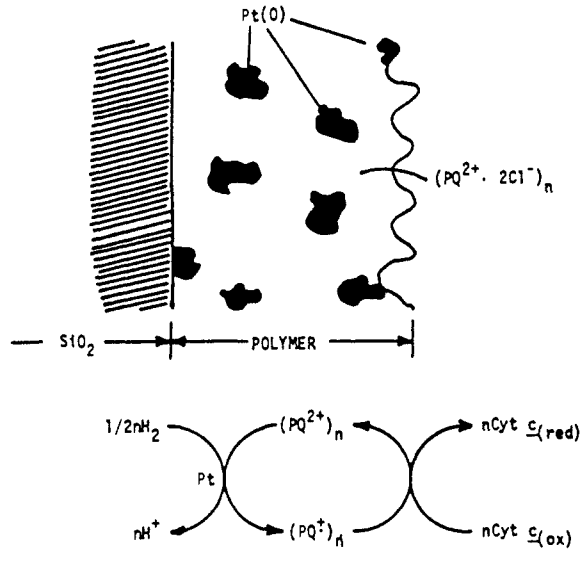

Previous work in this laboratory demonstrated the feasibility of effecting the H_2 reduction chemistry represented by Scheme I with a redox polymer/noble metal assembly as the catalyst deposited on the inside of ordinary Pyrex test tubes. The redox polymer used, $(PQ^{2+/+})_n$, is derived from an *N,N'*-dialkyl-4,4'-bipyridinium monomer I, and the noble metal M can be dispersed

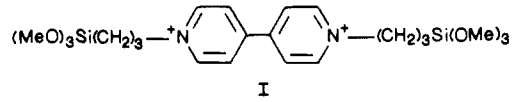

I

(1) (a) Brown, G. L. *Arch. Biochem. Biophys.* **1954**, *49*, 303. (b) Gygax, H. R.; Jordan, J. *Discuss. Faraday Soc.* **1968**, *45*, 227. (c) Knobloch, E. *Methods Enzymol.* **1971**, *18B*, p. 374. (d) Ostrowski, W.; Krawczyk, A. *Acta Chem. Scand.* **1963**, *17* (Suppl), 241. (e) Duke, P. R.; Kust, R. N.; King, L. A. *J. Electrochem. Soc.* **1969**, *116*, 32. (f) Dryhurst, G.; Kadish, K. M.; Scheller, F.; Renneberg, R. *Biological Electrochemistry*; Academic: New York, 1982; Vol. 1, p 398.

(2) (a) Durliat, H.; Comtat, M. *Anal. Chem.* **1982**, *54*, 856. (b) Heineman, W. R.; Hawkridge, F. M.; Blount, H. N. In *Electroanalytical Chemistry*; Bard, A. J., Ed., Marcel Dekker: New York, 1984, Vol. 13, p 1.

(3) (a) Szentrimay, R.; Yeh, P.; Kuwana, T. *ACS Symp. Ser.* **1977**, *38*, 143. (b) Heineman, W. R.; Meckstroth, M. L.; Norris, B. J.; Su, C.-H. *Bioelectrochem. Bioenerg.* **1979**, *6*, 577. (c) Kuwana, T.; Heineman, W. R. *Acc. Chem. Res* **1976**, *9*, 241. (d) Margoliash, E.; Schejter, A. *Adv. Protein Chem.* **1966**, *21*, 113. (e) Landrum, H. L.; Salmon, R. T.; Hawkridge, F. M. *J. Am. Chem. Soc.* **1977**, *99*, 3154. (f) Yeh, P.; Kuwana, T. *Chem. Lett.* **1977**, 1145. (g) Eddowes, M. J.; Hill, H. A. O.; Uosaki, K. *Bioelectrochem. Bioenerg.* **1980**, *7*, 527. (h) Albery, W. J.; Eddowes, M. J.; Hill, H. A. O.; Hillman, A. R. *J. Am. Chem. Soc.* **1981**, *103*, 3904.

(4) (a) Bookbinder, D. C.; Lewis, N. S.; Wrighton, M. S. *J. Am. Chem. Soc.* **1981**, *103*, 7656. (b) Bookbinder, D. C. Ph.D. Thesis, Massachusetts Institute of Technology, Cambridge, MA, 1982. (c) Chao, S. Ph.D. Thesis, Massachusetts Institute of Technology, Cambridge, MA, 1985.

0002-7863/88/1510-2270$01.50/0

Table I. Relevant Physical Properties of Heme Proteins

protein (MW) [source]	redox symbol	active site ($E^{o\prime}$ vs SCE, pH 7.0)	diffusn coeff, $cm^2\ s^{-1}$	self-exchange rate const, $M^{-1}\ s^{-1}$	λ_{max}, nm (ϵ_M, $M^{-1}\ cm^{-1}$)	physiolog functn
cytochrome *c* (12 300) [horse heart][a,b]	cyt c_{ox}/cyt c_{red}	$Fe^{3+/2+}$-heme (0.020 V)	1.2×10^{-6}	10^3–10^5	ox. 526 (1.10×10^4) red. 550, 550 (2.80×10^4)	electron carrier
myoglobin (17 816) [sperm whale][a,c]	Mb_{ox}/Mb_{red}	$Fe^{3+/2+}$-heme (−0.236 V)	1.0×10^{-6}	4×10^{-2}	ox. 503 (9.5×10^3), 632 red. 566 (1.18×10^4)	oxygen-transport agent
peroxidase (40 500) [horseradish][a,d,e]	POD_{ox}/POD_{red}	$Fe^{3+/2+}$-heme (−0.310 V)	7.0×10^{-7}		ox. 497 (1.00×10^4), 642 red. 558 (1.12×10^4)	H_2O_2 decomposition enzyme

[a] Dryhurst, G.; Kadish, K. M.; Scheller, F.; Renneberg, R. *Biological Electrochemistry*; Academic: New York, 1982; p 398. Kirshenbaum, D. M. *Atlas of Protein Spectra in the Ultraviolet and Visible Regions*; Plenum: New York, 1972. [b] Bowden, E. F.; Hawkridge, F. M.; Chlebowski, J. F.; Bancroft, E. E.; Thorpe, C.; Blount, H. N. *J. Am. Chem. Soc.* **1982**, *104*, 7641. [c] Antonini, E.; Brunori, M. *Hemoglobin and Myoglobin in Their Reactions with Ligands*; North Holland: Amsterdam, 1971; p 17. Riveros-Moreno, V.; Wittenberg, J. B. *J. Biol. Chem.* **247**, *1972*, 895. [d] Keilin, D.; Hartree, E. F. *Biochem. J.* **1951**, *49*, 88, 105. [e] Saunders, B. C.; Holmes-Siedle, A. G.; Stark, B. P. *Peroxidases*; Butterworth: Washington, 1964.

in the surface-bound polymer by first exchanging the halide anions of the polymer with MCl_4^{2-} (M = Pd, Pt) followed by reduction to produce elemental M.[5,6] The catalytic reduction of horse heart ferricytochrome *c* with H_2 using M = Pt was demonstrated to establish the concept, but the relatively small available surface area of the catalyst system on a flat glass substrate gives relatively slow rates of reaction. Accordingly, we have extended our work with such catalysts to systems having much larger surface area by immobilizing the catalyst assembly onto high surface area SiO_2 as a support. The strategy of high surface area SiO_2 catalysts can improve the available surface area by as much as 10^5 for ~3.0-mL solutions contained in 13 × 100 mm test tubes, leading to good absolute rates of catalytic reduction.

In addition to catalytic reduction of horse heart ferricytochrome *c* previously reported,[4] we include here results showing rapid reduction of the heme centers in sperm whale myoglobin and horseradish peroxidase, systems difficult or impossible to reduce in derivatized test tubes.[4b] Relevant properties of the redox reagents used in this work are given in Table I. Additionally, our work has been extended to include use of the cobalticenium reagent II[7] as a redox polymer, $[Co(CpR)_2^{+/0}]_n$, precursor.

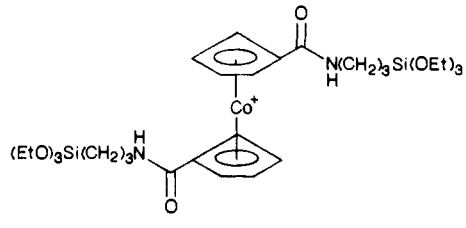

II

Further, the use of Pd, as well as Pt, as the noble metal has been demonstrated. The formal potentials of the redox polymers from I[4] and II[7] are known to be pH independent and have about the same value, about −0.6 V vs SCE. Thus, aqueous H_2 solutions of pH greater than about pH 6 are capable of fully reducing the immobilized redox centers, on thermodynamic grounds. Reduction of the heme centers of cytochrome *c*, myoglobin, or peroxidase are all possible with the reduced form of the polymers derived from I or II, considering their formal potentials (Table I). Finally, preparation of catalysts having the structured arrangement illustrated in Scheme II is demonstrated, with the objective being to "bury" the noble metal so that the biological reagent contacts only the redox polymer derived from I or II. A communication describing the use of the high surface area $[SiO_2]$–$(PQ^{2+}\cdot 2Cl^-\cdot Pt)_n$ catalysts for the regeneration of NADH from NAD^+ using H_2

Scheme II. Structured Catalyst for the Equilibration of One-Electron Biological Redox Molecules with the H_2O/H_2 Redox Couple[a]

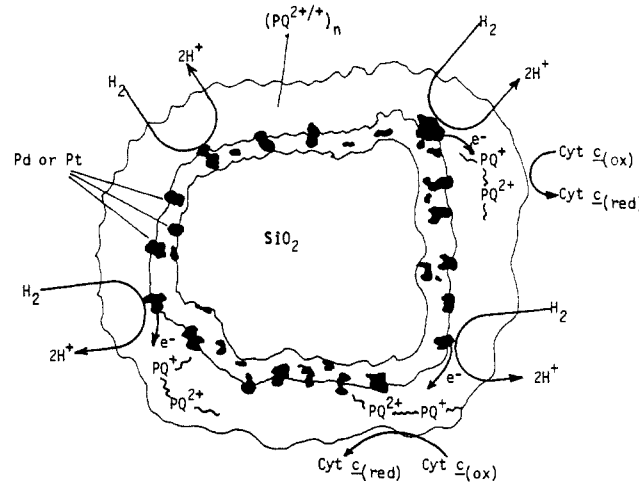

[a] The noble metal, Pt or Pd, responsible for activating the H_2 is "buried" by the overcoat of redox polymer $(PQ^{2+/+})_n$ or $(Co(CpR)_2^{+/0})_n$. This catalyst is referred to as a type 2 catalyst in this work.

Scheme III. General Synthetic Procedure for Preparation of the Catalysts for the Process Represented by Scheme I

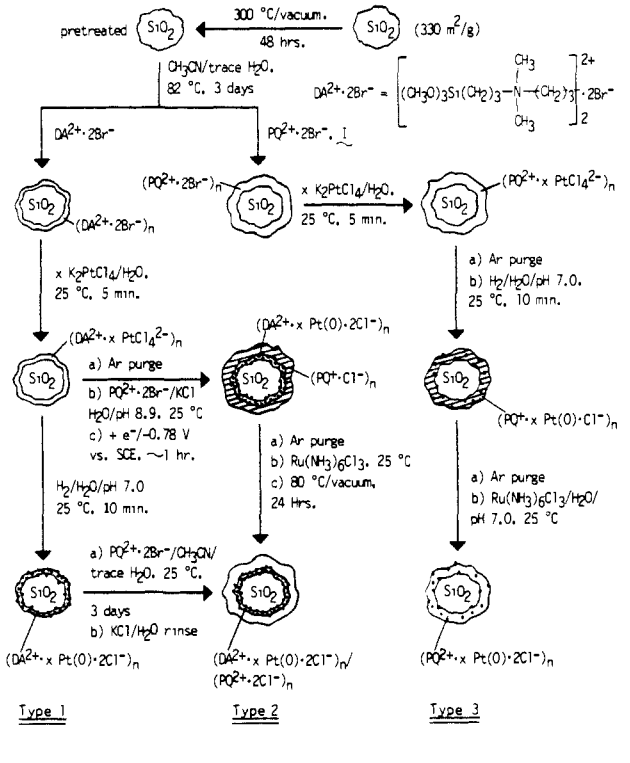

(5) Bruce, J. A.; Murahashi, T.; Wrighton, M. S. *J. Phys. Chem.* **1982**, *86*, 1552.

(6) (a) Bookbinder, D. C.; Wrighton, M. S. *J. Am. Chem. Soc.* **1980**, *102*, 5123. (b) Bookbinder, D. C.; Bruce, J. A.; Dominey, R. N.; Lewis, N. S.; Wrighton, M. S. *Proc. Natl. Acad. Sci. U.S.A.* **1980**, *77*, 6280. (c) Dominey, R. N.; Lewis, N. S.; Bruce, J. A.; Bookbinder, D. C.; Wrighton, M. S. *J. Am. Chem. Soc.* **1982**, *104*, 467. (d) Bruce, J. A.; Wrighton, M. S. *J. Am. Chem. Soc.* **1982**, *104*, 74.

(7) Simon, R. A.; Mallouk, T. E.; Daube, K. A.; Wrighton, M. S. *Inorg. Chem.* **1985**, *24*, 3119.

Table II. Representative Composition and Coverage Characterizations of Catalysts

catalyst	x	surface area,[a] $cm^2/10$ mg	Γ,[b] mol/cm^2		
			PQ^{2+}	DA^{2+}	Pt
type 1 $[SiO_2]$-$(DA^{2+}\cdot 2Cl^-\cdot xPt)_n$	1	3.0×10^4	none present	5.2×10^{-11}	5.2×10^{-11}
	trace[c]		none present	5.2×10^{-11}	6×10^{-12}
type 2 $[SiO_2]$-$(DA^{2+}\cdot 2Cl^-\cdot xPt_n/(PQ^{2+}\cdot 2Cl^-)_n$	1	2.1×10^4	1.9×10^{-10}	5.2×10^{-11}	5.2×10^{-11}
type 3 $[SiO_2]$-$(PQ^{2+}\cdot 2Cl^-\cdot xPt)_n$	1	7.8×10^3	1.5×10^{-9}	none present	1.5×10^{-9}
	trace[c]		1.5×10^{-9}	none present	2×10^{-11}

[a] Calculations based on 330 m^2/g for the underivatized SiO_2 as supplied. The variations in these values are due to differences in the SiO_2 weight percent in the three types of finished catalysts. The entries are considered to be upper limits since the actual derivatized surface area depends on the accessibility of internal pores of SiO_2 by I and III. [b] Calculations based on the assumption that the surface area of the SiO_2 is 330 m^2/g and on the elemental analysis of N, a unique element from derivatization with I or III. [c] For x = trace, a 30-mg portion of the derivatized SiO_2 powder was added to 0.1 mg of K_2PtCl_4 dissolved in 10 mL of H_2O. The entries are calculated assuming that all $PtCl_4^{2-}$ exchanged into the polymer and therefore must be considered to be the upper limits.

and lipoamide dehydrogenese has been published recently.[8]

Results and Discussion

a. Preparation and Characterization of Catalysts. Three general types of polymer/noble metal catalyst assemblies have been prepared on high surface area SiO_2. The essential features of the three types of catalysts and synthetic procedures are illustrated in Scheme III. Type 3 catalysts involve derivatizing the SiO_2 in a manner that leads to a redox polymer into which the noble metal is dispersed throughout, $[SiO_2]$-(polymer·M), and type 2 catalysts are ones where the noble metal is buried under the redox polymer, $[SiO_2]$-$(DA^{2+}\cdot 2Cl^-\cdot xM)_n$/(polymer). In these representations of the catalysts, "polymer" is redox material derived from hydrolysis of I or II, $(PQ^{2+/2})_n$ or $(Co(CpR)_2^{+/0})_n$, respectively; $(DA^{2+}\cdot 2Cl^-)_n$ is the polymer derived from hydrolysis of the $Si(OR)_3$ groups on the aliphatic diammonium monomer represented by III; and M is the noble metal Pd or Pt. The general

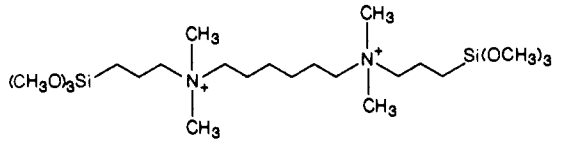

III

method of synthesis of the catalysts is outlined in Scheme III for those catalysts employing Pt and the polymers from I and/or III. Catalysts prepared from the polymers derived from II, III, and Pt or Pd and the catalysts from I, III, and Pd have been prepared according to similar procedures.

The synthetic procedure for all catalysts begins with commercially available SiO_2 obtained with a surface area of 330 m^2/g. The SiO_2 was generally pretreated prior to functionalization by heating in a vacuum ($\sim 10^{-3}$ Torr) at 300 °C for 48 h. Type 3 catalysts, $[SiO_2]$-(polymer·M), can be prepared by derivatizating the pretreated SiO_2 with I or II. After derivatization with I the powders are colorless to pale yellow, and the powders after derivatization with II are yellow, consistent with the known spectral properties of the monomers I[4,9] and II.[7] The next step is to introduce the noble metal into the surface-confined polycation by exchanging the charge-compensating anions for MCl_4^{2-}. The dry powder is orange to red, characteristic of MCl_4^{2-} at this stage.[10] Finally, the MCl_4^{2-} is reduced by purging an aqueous suspension of the derivatized SiO_2 with H_2 gas at 25 °C. The evidence that MCl_4^{2-} becomes reduced is that the powders become intensely blue-violet when the redox polymer is that from reagent I.[4] The color changes associated with the polymer from II are somewhat more difficult to discern, because the intensities of the absorptions are less[7] and the oxidized form is yellow and the reduced form of the polymer is red.[7] Nonetheless, color changes associated with reduction of polymers from I or II are visible to the naked eye when MCl_4^{2-}-compensated polymers are exposed to H_2 in aqueous solution containing no other species. Under the same conditions, SiO_2 derivatized with polymers from I or II but, without M or MCl_4^{2-}, undergo no visible spectral changes in the presence of H_2. As synthesized, the $[SiO_2]$-(polymer·M) yields a material that has the polymer in its reduced state and is, therefore, O_2 sensitive.[11] In the presence of H_2O the reaction of the reduced polymer with O_2 likely yields H_2O_2, which can lead to degradation of the polymer. Accordingly, the $[SiO_2]$-(polymer·M) is equilibrated with $Ru(NH_3)_6^{3+}$ in aqueous solution to oxidize the polymer. Reaction of the reduced forms of the polymers from I or II with $Ru(NH_3)_6^{3+}$ is known to occur rapidly.[12,13] The resulting $[SiO_2]$-(polymer·M) is then in its oxidized state and can be handled in air. The catalyst can be separated from the preparation solutions by filtration.

The amount of M dispersed in the redox polymer can be controlled by limiting the extent of ion exchange. Earlier experiments established that complete exchange of halide anions of the polymers derived from I[6d] or II[7] will be achieved when the polymer is equilibrated in an aqueous solution containing a sufficient concentration of anionic transition-metal complexes like those employed here to introduce the elemental noble metals. The strong binding of large, anionic transition-metal complexes relative to halides and other small inorganic anions into surface-bound polycations is now a general result[6d,7,14-17] that can be exploited in the sort of synthesis described here. For the polymer derived from I the incorporation of one M atom per monomer is expected based on the 2^+ charge of the monomer and the 2^- charge of the MCl_4^{2-}. For the polymer derived from II one M atom for every two monomers is expected since the monomer II has only a $1+$ charge. By using a deficiency of MCl_4^{2-} it is possible to obtain less than these stoichiometric quantities of M in the polymer. For the combination of I and Pt two extremes have been prepared, and materials prepared by using a trace of $PtCl_4^{2-}$ and an excess of $PtCl_4^{2-}$ are illustrative, as data in Table II show.

The type 2 catalyst involves covering the noble metal with the redox polymer. For this type of catalyst the first functionalization step is to derivatize the SiO_2 with reagent III, giving a colorless powder. The charge-compensating Cl^- anions are then exchanged by excess or trace MCl_4^{2-} by suspending the SiO_2 derivatized when III in an aqueous solution and adding K_2MCl_4 (M = Pd, Pt). Results of a study of the binding of large, complex anions into the polymer from III and related monomers will be published elsewhere.[18] The resulting $[SiO_2]$-$(DA^{2+}\cdot xMCl_4^{2-})_n$ is then

(8) Chao, S.; Wrighton, M. S. *J. Am. Chem. Soc.* **1987**, *109*, 5886. Cf. also: Thanos, I.; Simon, H. *Angew. Chem., Int. Ed. Engl.* **1986**, *25*, 462.
(9) Bookbinder, D. C.; Wrighton, M. S. *J. Electrochem. Soc.* **1983**, *130*, 1080.
(10) Chatt, J.; Gamlen, G. A.; Orgel, Z. E. *J. Chem. Soc.* **1958**, 486.
(11) (a) Thorneley, R. N. F. *Biochim. Biophys. Acta* **1974**, *33*, 487. (b) Summers, L. A. *The Bipyridinium Herbicides*; Academic: London, 1980; p 328.
(12) Lewis, T. J.; White, H. S.; Wrighton, M. S. *J. Am. Chem. Soc.* **1984**, *106*, 6947.
(13) Mallouk, T. E.; Cammarata, V.; Crayston, J. A.; Wrighton, M. S. *J. Phys. Chem.* **1986**, *90*, 2150.
(14) Dominey, E. N.; Lewis, T. J.; Wrighton, M. S. *J. Phys. Chem.* **1983**, *87*, 5345.
(15) Walter, B. *Anal. Chem.* **1983**, *55*, 498A.
(16) (a) Carr, P. W.; Bower, L. D. *Immobilized Enzymes in Analytical and Clinical Chemistry*; Wiley-Interscience: New York, 1980. (b) Fishman, M. M. *Anal. Chem.* **1980**, *52*, 152R.
(17) Chao, S.; Robbins, J. L.; Wrighton, M. S. *J. Am. Chem. Soc.* **1983**, *105*, 181.

collected by centrifugation and washed with pure H_2O to remove any excess K_2MCl_4. At this point the dry powder is the orange to red of the MCl_4^{2-} ion. To reduce the surface-bound MCl_4^{2-}, the powder is suspended in pure H_2O and the heterogeneous mixture is purged with H_2 gas at 25 °C until the powder turns gray, consistent with the formation of the dispersed elemental Pt or Pd. The resulting $[SiO_2]$-$(DA^{2+}\cdot 2Cl^-\cdot xM)_n$ can be used as a catalyst (type 1) for comparison with the catalyst materials involving the redox polymers. The $[SiO_2]$-$(DA^{2+}\cdot 2Cl^-\cdot xM)_n$ can be derivatized with the redox monomer I or II to give a surface-confined redox polymer that coats an inner layer of the electroinactive polymer from III into which the noble metal is dispersed as illustrated in Scheme III. As the data in Table II illustrate, the amount of $(DA^{2+})_n$ confined to the SiO_2 can be very small. Assuming that the SiO_2 surface area remains 330 m^2/g, the coverage is less than a monolayer for the case shown in Table II. However, the amount of $(DA^{2+})_n$ is sufficient to allow the immobilization of the noble metal, since the gray color due to the elemental metal can be seen after H_2 reduction of the surface-bound MCl_4^{2-}. Generally, coverage can be varied by changing the derivatization times.

The $[SiO_2]$-$(DA^{2+}\cdot 2Cl^-\cdot xM)_n$ can be derivatized with I or II by merely reacting the powder suspended in a solution of I or II. However, another route can be used to produce the surface-bound polymer from I, based on knowledge stemming from the derivatization of electrode surfaces.[8] The electrochemical procedure to modify electrodes involves reducing the monomer I in aqueous solution at the electrode. The reduced form of I is much less soluble and precipitates onto the electrode, resulting in more rapid polysiloxane formation. The deposition of polymer onto $[SiO_2]$-$(DA^{2+}\cdot 2Cl^-\cdot xM)_n$ can also be reductively assisted by suspending the powder in an aqueous solution of I and exposing the mixture to H_2 for reduction of the viologen without stirring. Alternatively, electrochemical reduction of the viologen can be used to effect derivatization of the SiO_2. The functionalization of the powder with the reduced polymer results. The surface-confined, reduced polymer can be oxidized with $Ru(NH_3)_6^{3+}$, as described above, to yield the desired catalyst that can be handled without decomposition in air.

It is difficult to establish that the noble metal is actually buried by the redox polymer in the catalyst assembly represented by Schemes II and III. However, the method of synthesis is consistent with the structure claimed. It is expected that the interface is one that exposes no clean noble metal to a solution containing a large biological redox reagent. Rather, the buried noble metal based catalysts only expose the redox polymer to a large biological redox molecule. The successful preparation of the essential structural feature of a buried noble metal with the redox polymer overcoat can be demonstrated on planar surfaces of conductors. For example, Figure 1 illustrates the intensity of Auger electron intensities associated with several elements while sputtering through an interface constructed according to the sort of procedure given in Scheme III for a type 2 catalyst. In this case the substrate is a single crystal Si surface having a thin SiO_2 layer that is first derivatized with III and ion exchanged with $PdCl_4^{2-}$ to yield Si/SiO_2-$(DA^{2+}\cdot PdCl_4^{2-})_n$. The surface is then immersed in H_2O and reduced with H_2 to form the elemental Pd. Finally, the surface is derivatized with II in the same manner used to derivatize the high surface area $[SiO_2]$-$(DA^{2+}\cdot 2Cl^-\cdot Pd)_n$ materials. As can be seen in the so-called depth profile analysis shown in Figure 1, the interface is structured in the manner indicated in Schemes II and III for the type 2 catalyst and no noble metal is detectable at the outermost surface of the polymer. Unfortunately, the insulating, small SiO_2 particles comprising the high surface area catalysts cannot be similarly characterized, but the structural evidence from derivatization of planar Si/SiO_2 surfaces is compelling proof of the structure expected for type 2 catalysts based on the synthetic procedure.

(18) (a) Simon, R. A.; Wrighton, M. S., to be submitted for publication. (b) Simon, R. A. Ph.D. Thesis, Massachusetts Institute of Technology, Cambridge, MA, 1984.

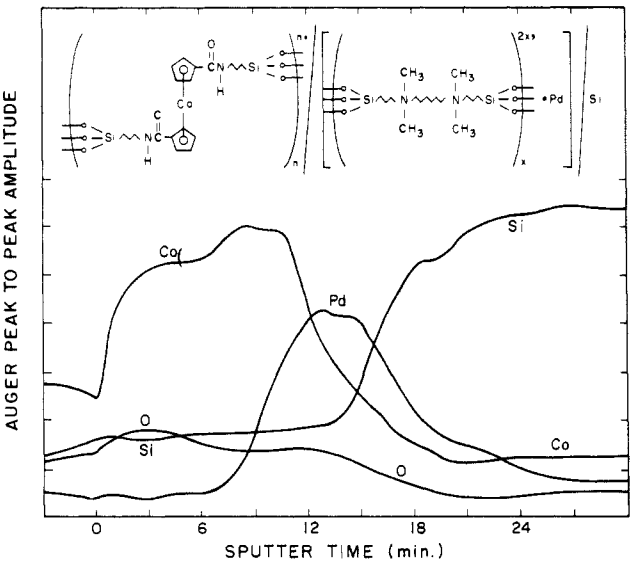

Figure 1. Auger/depth profile analysis for a planar Si/SiO_2 surface prepared as in Scheme III by using polymer derived from III, Pd incorporation, and functionalization with the redox polymer derived from II.

The modification of SiO_2 with reagents such as I–III can proceed in good yield. The yields (percent starting solution monomer that is attached to the surface) for these derivatization reactions are, in general, better than 70%. The final surface polymer coverage can be easily controlled by changing the ratio of SiO_2 to monomer. However, significant coverage, at least in excess of one-tenth of a single monolayer ($\sim 10^{-11}$ mol/cm^2), is necessary to retain the MCl_4^{2-} anions[19] that are loaded and subsequently reduced to form M for catalyzing the redox equilibration with molecular H_2. Derivatized SiO_2 with smaller coverages were found to be unable to bind MCl_4^{2-}. Representative polymer coverages as a result of our preparations are included in Table II.

As an essential final step of their synthesis, the catalysts must be rinsed through repeated centrifuge and decant cycles with high-purity H_2O, followed by CH_3CN, and then heated to 80 °C under vacuum for 24 h. Under such treatment, any possible physically adsorbed siloxane oligomer is washed away, and the bound polymer likely undergoes further cross-linking at the higher temperature. The resulting catalysts involve covalently bonded PQ^{2+}, DA^{2+} or $Co(CpR)_2^+$ centers persistently anchored to the surface of SiO_2 and M. This fact is established for the $(PQ^{2+})_n$ type 2 and type 3 catalysts by a simple control experiment. In the procedure, 2 mL of UV-grade H_2O is added to 0.1 g of one of the catalysts in a 1.0-cm cuvette. The suspension is then subjected to continuous mechanical stirring with a Teflon-coated magnetic stirring button for $\sim$1 h and centrifuged, giving a clear solution. After the cuvette is carefully lowered into a scanning UV–vis spectrophotometer without disturbing the settled particulates, a spectrum is recorded. The absence of an absorption band in the $\sim$260-nm region (OD $\ll$0.01) indicates that the supernatant is essentially free of leached PQ^{2+}, which has a large ϵ_{260nm} 3×10^4 M^{-1} cm^{-1}.[9] It is important to verify that this solution species does not exist in even very minute quantities. This precaution is necessary since even <1 μM of leached PQ^{2+} could still bring about a mechanism for the reduction of biological molecules that involves the intermediacy of a solution mediator. Our intention is to develop surface-bound mediators for equilibrating the biological molecules with the surface.

b. Reduction of Cytochrome *c*, Myoglobin, and Peroxidase with H_2 Using Type 1–3 Catalysts. Table III gives data concerning the activities of the high surface area type 1–3 catalysts for the reduction of cytochrome *c* (cyt c_{ox}), myoglobin (Mb_{ox}), and

(19) Ricco, A. J. Ph.D. Thesis, Massachusetts Institute of Technology, Cambridge, MA, 1984.

Table III. Results of Heme Protein Reduction Catalyzed by Type 1–3 Catalysts

catalysts (amt used, mg)[a]	starting soln	final soln	yield, %	reactn time, min[b]
	Cytochrome *c* Reductions			
type 3 $[SiO_2]$-$(PQ^{2+}\cdot 2Cl^-\cdot$trace Pt$)_n$ (10)	39 μM cyt c_{ox}/H_2	40 μM cyt c_{red}[d]	100	<5
	1.6 mM cyt c_{ox}/H_2	1.6 mM cyt c_{red}	100	<5
type 3 $[SiO_2]$-$(PQ^{2+}\cdot 2Cl^-\cdot Pt)_n$ (10)	39 μM cyt c_{ox}/H_2	14 μM cyt c_{red}	36	<5
	2.6 mM cyt c_{ox}/H_2	2.6 mM cyt c_{red}	100	<5
type 2 $[SiO_2]$-$(DA^{2+}\cdot 2Cl^-\cdot Pt)_n/(PQ^{2+}\cdot 2Cl^-)_n$ (10)	39 μM cyt c_{ox}/H_2	39 μM cyt c_{red}	100	<5
type 2 $[SiO_2]$-$(DA^{2+}\cdot 2Pt\cdot 2Cl^-)_n/(Co(CpR)_2^+\cdot Cl^-)_n$ (8)	100 μM cyt c_{ox}/H_2	~100 μM cyt c_{red}	~100	<5
Pt black (100)[c]	50 μM cyt c_{ox}/Ar[e]	7 μM cyt c_{ox}[e]	*e*	<5[e]
	50 μM cyt c_{ox}/H_2	7 μM cyt c_{red}	14	<5
	Myoglobin Reductions			
type 3 $[SiO_2]$-$(PQ^{2+}\cdot 2Cl^-\cdot$trace Pt$)_n$ (10)	50 μM Mb_{ox}/H_2	48 μM Mb_{red}	96	<5
	0.6 mM Mb_{ox}/H_2	0.6 mM Mb_{red}	100	<5
type 2 $[SiO_2]$-$(DA^{2+}\cdot 2Pt\cdot 2Cl^-)_n/(Co(CpR)_2^+\cdot Cl^-)_n$ (8)	100 μM Mb_{ox}/H_2	~100 μM Mb_{red}[f]	~100	<5
type 1 $[SiO_2]$-$(DA^{2+}\cdot 2Cl^-\cdot$trace Pt$)_n$ (10)	127 μM Mb_{ox}/H_2	122 μM Mb_{red}	96	~80
Pt black (100)[c]	72 μM Mb_{ox}/Ar[e]	<1 μM Mb_{ox}[e]	*e*	<5
	72 μM Mb_{ox}/H_2	<1 μM Mb_{red}	~0	<5
	Peroxidase Reductions			
type 3 $[SiO_2]$-$(PQ^{2+}\cdot 2Cl^-\cdot$trace Pt$)_n$ (10)	74 μM POD_{ox}/H_2	75 μM POD_{red}[g]	100	<5
type 2 $[SiO_2]$-$(DA^{2+}\cdot 2Cl^-\cdot Pt)_n/(PQ^{2+}\cdot 2Cl^-)_n$ (10)	74 μM POD_{ox}/H_2	73 μM POD_{red}	99	<5
type 2 $[SiO_2]$-$(DA^{2+}\cdot 2Cl^-\cdot Pt)_n/(Co(CpR)_2^+\cdot Cl^-)_n$ (8)	90 μM POD_{ox}/H_2	~90 μM POD_{red}	~100	~15
type 1 $[SiO_2]$-$(DA^{2+}\cdot 2Cl^-\cdot$trace Pt$)_n$ (10)	73 μM POD_{ox}/H_2	73 μM POD_{ox}	0	>250

[a] Typically, 8–100 mg of catalyst in a 1-cm path length quartz cuvette was suspended in 3.0 mL of the starting solution under 1 atm H_2. The mixture was then centrifuged, and the final solution composition and concentration were determined by UV-Vis spectroscopy. [b] <5 min refers to the time used to process the solution after the initial H_2 purge. [c] Pt black has ~10 m^2 surface area/g of catalyst as specified by the commercial supplier, Johnson-Matthey. [d] Figure 2. [e] In this experiment, under Ar, the protein adsorbs onto the Pt black. Presumably the loss in detectable protein is due to retention on the Pt. Under H_2, the loss in total protein concentration is attributed to adsorption. [f] Figure 3. [g] Figure 4.

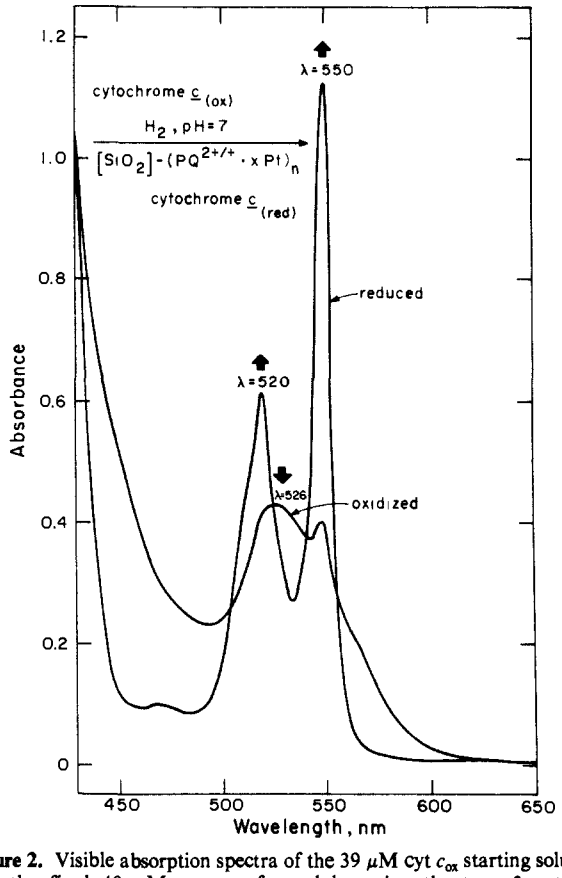

Figure 2. Visible absorption spectra of the 39 μM cyt c_{ox} starting solution and the final 40 μM cyt c_{red} formed by using the type 3 catalyst $[SiO_2]$-$(PQ^{2+}\cdot 2Cl^-\cdot$trace Pt$)_n$ under H_2.

peroxidase (POD_{ox}). Comparison data for naked, high surface area Pt are also included. Figures 2–4 show spectral data establishing the clean reduction of cyt c_{ox}, Mb_{ox}, and POD_{ox} using the type 2 or 3 catalysts under H_2. Data in Table III are for Pt as the noble metal. Some results have been obtained for Pd also and there seem to be no substantive differences, though detailed comparisons have not been made.

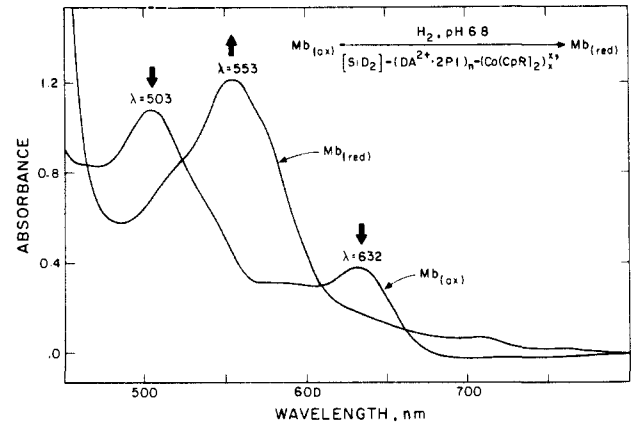

Figure 3. Visible absorption spectra of the 100 μM Mb_{ox} starting solution and the ~100 μM Mb_{red} formed by using the type 2 catalyst $[SiO_2]$-$(DA^{2+}\cdot 2Pt)_n/(Co(CpR)_2^+\cdot Cl^-)_n$ under H_2.

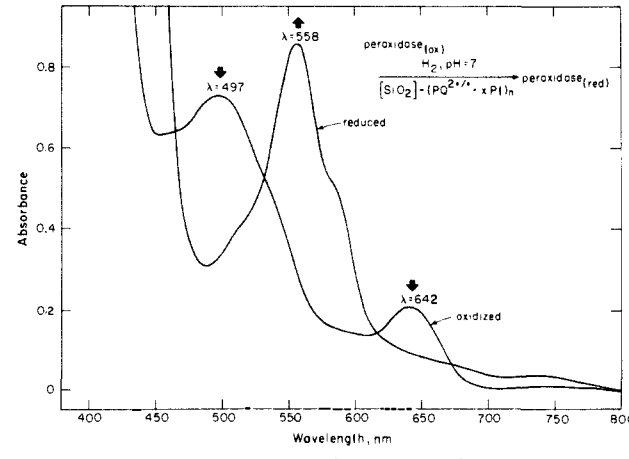

Figure 4. Visible absorption spectra of the 75 μM POD_{ox} starting solution and the ~75 μM POD_{red} formed by using the type 3 catalyst $[SiO_2]$-$(PQ^{2+}\cdot 2Cl^-\cdot$trace Pt$)_n$ under H_2.

As expected, observed rates for the reduction of 39 μM–2.6 mM cyt c_{ox} to give completely reduced cyt c_{red} solutions are fast

for all the type 2 and 3 cases. Consistent with the electrochemical characterizations that confirm cyt *c* adsorption on naked Pt surfaces, however, the type 3 catalyst $[SiO_2]$–$(PQ^{2+}\cdot 2Cl^-\cdot Pt)_n$, which is highly loaded with Pt, could only generate 14 μM cyt c_{red} and no cyt c_{ox} from 39 μM cyt c_{ox}. The remaining cyt c_{red} "missing" from solution presumably adsorbed onto the Pt surface and hence is not detectable by our optical spectroscopic technique. This problem for the type 3 catalyst can be solved by using a type 3 catalyst loaded with only a trace amount of Pt, $[SiO_2]$–$(PQ^{2+}\cdot 2Cl^-\cdot$trace Pt$)_n$ (Figure 2). Alternatively, a type 2 bilayer catalyst, $[SiO_2]$–$(DA^{2+}\cdot 2Cl^-\cdot Pt)_n/(PQ^{2+}\cdot 2Cl^-)_n$, where Pt is only present within the inner $(CA^{2+})_n$ layer can also be used. The 100% yield obtained from using these two catalysts in the reduction of 39 μM cyt c_{ox} (Table III) is proof for the effectiveness of the $(PQ^{2+})_n$ layer in overcoming the problem of cyt *c* adsorption on Pt. In contrast, a suitable quantity of Pt black providing similar active surface area gave rise to a loss of 43 μM cyt c_{red} due to adsorption when used to catalyze the reduction of 50 μM cyt c_{ox} under the same reaction conditions. At higher cyt *c* concentrations, in the millimolar range, with the amount of available Pt surface kept constant, the loss of cyt *c* due to adsorption becomes relatively small and cannot be readily detected by optical spectroscopy due to the overwhelmingly high cyt *c* concentration in solution. The reduction of a 10-mL solution of 5 mM cyt c_{ox} using 3 mg of $[SiO_2]$–$(PQ^{2+}\cdot 2Cl^-\cdot$trace Pt$)_n$ under H_2 represents a turnover number of >10 per PQ^{2+} unit for the catalyst. This number is considered a lower limit, since the recovered catalyst has been found to be still active.

As reported in Table III, fast reduction of 50 μM and 0.6 mM Mb_{ox} can both be effected by the use of the type 3 catalyst $[SiO_2]$–$(PQ^{2+}\cdot 2Cl^-\cdot$trace Pt$)_n$ under H_2 to give the desired Mb_{red} in 100% yield. Our result here is different from the results using a derivatized test tube, glass–$(PQ^{2+}\cdot 2Cl^-\cdot Pt)_n$, as the catalyst.[4] There, attempts to reduce Mb_{ox} at $\geq$50 μM failed, presumably due to the severe blocking of the small surface area available for reaction. In the present work, slight loss in concentration (<5%) occurred during the reduction of 50 μm Mb_{ox} with the type 3 catalyst $[SiO_2]$–$(PQ^{2+}\cdot 2Cl^-\cdot$trace Pt$)_n$ that yielded 48 μM Mb_{red}. Nonetheless, the time required for complete reduction was still <5 min. This reflects an improvement over the time (~2 h) needed previously[4] when employing the derivatized test tubes having small available surface area. Figure 3 shows that the type 2 catalyst $[SiO_2]$–$(DA^{2+}\cdot 2Cl^-\cdot Pt)_n/(Co(CpR)_2^+\cdot Cl^-)_n$ is effective in reducing ~100 μM Mb_{ox} in <5 min.

The heterogeneous rate constant for reduction of Mb_{ox} at naked metal surfaces, k_{het}, is so small,[20] and so far below the detection limits of conventional electrokinetic techniques, that a meaningful value of k_{het} can not be found in the literature. For all practical purposes, it is widely held that Mb_{ox} is inactive at the untreated solid conductor interfaces. However, this apparently applies only to low surface area materials. As can be seen in Table III, Mb_{ox} can be reduced (at least to a small extent) to Mb_{red} not only at the bare surfaces of high surface area Pt black but also at the type 1 catalyst $[SiO_2]$–$(DA^{2+}\cdot 2Cl^-\cdot Pt)_n$, which has a high density of Pt particles exposed to the solution. But as we have expected, the yield of Mb_{red} dropped significantly due to the loss of the Mb_{red} from solution owing to adsorption on Pt (from 72 to <1 μM on Pt black). Such a deleterious side effect will remain as long as a large amount of bare Pt surface is exposed to the protein solution. As reported in Table III, the type 1 catalyst $[SiO_2]$–$(DA^{2+}\cdot 2Cl^-\cdot$trace Pt$)_n$ with only a small amount of Pt can catalyze the reduction of 127 μM Mb_{ox} to 122 μM Mb_{red} and no Mb_{ox} in ~80 min. Because $(DA^{2+})_n$ is neither a conducting polymer nor a redox-active mediator, direct electron transfer from the supported Pt to Mb_{ox} in solution must occur. Furthermore, the reduction has evidently not suffered much from the ill-effect of adsorption. The exact reason(s) why the type 3 catalyst $[SiO_2]$–$(PQ^{2+}\cdot 2Cl^-\cdot$trace Pt$)_n$ and its structural analogue the type 1 catalyst $[SiO_2]$–$(DA^{2+}\cdot 2Cl^-\cdot$trace Pt$)_n$ can perform remarkably well against protein adsorption is not clear. Perhaps the exposed surface of the small number of Pt particulates in these catalysts is tightly surrounded by an abundance of $(PQ^{2+})_n$ or $(DA^{2+})_n$ polymer. As a result, the formation of the metal–ligand bonding between the protein NH_3^+ and SH functionalities and M may be hindered.

The enzyme horseradish peroxidase is so large that direct electron transfer involving its heme active site with smooth, naked, metal surfaces is difficult, if not impossible. No electrochemistry, aside from the reduction of the disulfide functionality at more negative potentials than $E^{\circ\prime} = -0.310$ V vs SCE at pH 7.0 for the Fe^{3+}/Fe^{2+}-heme active site of peroxidase has been observed.[21] Results from a random sampling of a variety of high surface area noble metal catalysts under H_2 were able to attest to the electrodic inertness of POD_{ox} at the bare surfaces. The catalysts we tested included 5% Pt, Pd, or Ir supported on SiO_2, and the POD_{ox} concentration of 87 μM was unchanged after >1 h under H_2. As reported in Table III, a 73 μM solution of POD_{ox} was also not affected under H_2 in the presence of the type 1 catalyst $[SiO_2]$–$(DA^{2+}\cdot 2Cl^-\cdot$trace Pt$)_n$ for >4 h.

Importantly, the type 2 and 3 catalysts can effect the reduction of POD_{ox} at high observed rates (Table III). Furthermore, the reduction of 75 μM POD_{ox} solutions catalyzed by the type 3 catalyst $[SiO_2]$–$(PQ^{2+}\cdot 2Cl^-\cdot$trace Pt$)_n$ (Figure 4) and the type 2 catalyst $[SiO_2]$–$(DA^{2+}\cdot 2Cl^-\cdot Pt)_n/(PQ^{2+}\cdot 2Cl^-)_n$ or –/$(Co(CpR)_2^+\cdot Cl^-)_n$ proceeds without the complication of concentration loss due to surface adsorption. The following control experiment was conducted to rule out the possibility that the reduction might have been catalyzed by leached PQ^{2+} or $Co(CpR)_2^+$ centers in solution. First, 10 mg of the catalyst was added to a 2.0-mL portion of an 82 μM POD_{ox} solution (prepared with deoxygenated aqueous phosphate buffer at pH 7.0). Under Ar, the resulting suspension was stirred for 1 h and filtered. The recovered filtrate containing any leached PQ^{2+} (or $Co(CpR)_2^+$) and the 82 μM POD_{ox} was then syringed into a cuvette containing 10 mg of $[SiO_2]$–$(DA^{2+}\cdot 2Cl^-\cdot Pt)_n$ under an Ar atmosphere. When subsequently placed under H_2, the POD_{ox} solution remained unaffected after >2 h, as shown by the optical spectra acquired periodically. The reduction of POD_{ox} would have occurred if any leached PQ^{2+}- or $Co(CpR)_2^+$-mediating species was present in the solution, because it has been demonstrated that $[SiO_2]$–$(DA^{2+}\cdot 2Cl^-\cdot Pt)_n$ will catalyze the reduction of solution PQ^{2+} under such conditions. The PQ^+ in solution would in turn reduce the biological reagents. The absence of leached redox species in solution was also confirmed by optical spectroscopy as described above in the detailed description of the preparation.

Conclusions

Results summarized in Table III and Figures 2–4 show that the high surface area catalysts of type 2 and 3 in Scheme III are effective in bringing about rapid, clean one-electron reduction of horse heart ferricytochrome *c*, sperm whale myoglobin, and horseradish peroxidase with H_2 as the reducing agent. H_2 is a convenient reducing agent because (1) it is routinely available in high purity, (2) the oxidation product H^+ is generally inconsequential in well-buffered solutions, and (3) excess H_2 is easily removed from the solution. Since the type 2 and 3 catalysts are solids, the catalyst materials are easily separated from the reaction mixture. For many biological redox systems H_2 represents adequate thermodynamic reducing power for the desired reduction processes. Thus, the use of H_2 to manipulate the state of charge of some biological electron-transfer reagents (Scheme I) appears to be attractive.

The catalysts for use according to Scheme I are easily prepared and represent a kind of synthetic hydrogenase. One catalyst component, the noble metal, activates the H_2, and the second component, the redox polymer, equilibrates with the M/H_2 and with the biological redox center. The molecular redox reagent

(20) (a) Stargardt, J. F.; Hawkridge, F. M.; Landrum, H. L. *Anal. Chem.* **1978**, *50*, 930. (b) Castner, J. F.; Hawkridge, F. M. *J. Electroanal. Chem.* **1983**, *143*, 217. (c) Bowden, E. F.; Hawkridge, F. M.; Blount, H. N. *J. Electroanal. Chem.* **1980**, *116*, 447.

(21) (a) Razumas, V. J.; Gudavicius, A. V.; Kulys, J. J. *J. Electroanal. Chem.* **1983**, *151*, 311. (b) Yaropolov, A. I.; Tarasevich, M. R.; Varfolomeev, S. D. *Bioelectrochem. Bioenerg.* **1978**, *5*, 18.

presumably provides a way to better interface the biological redox systems with the surface. The type 2 catalysts and the type 3 catalysts with low M incorporation preclude direct interaction of the biological reagents with the noble M. The noble metal under H_2 could effect catalytic hydrogenation of unsaturated sites and hydrogenolysis processes. While high surface area noble metals should be effective as catalysts for one-electron reduction processes, it is evident that such is not as efficient as the type 2 and 3 catalysts that we have developed. Indeed, the lack of activity toward horseradish peroxidase with high surface area M under conditions where the type 2 and 3 catalysts are effective demonstrates the superiority of the catalysts we have prepared.

Electrochemical methods have been used to show that reduction of horse heart ferricytochrome *c* with the reduced forms of the polymers from I or II occurs with large rate constants $>10^5$ M^{-1} s^{-1}.[22] Data are not yet available for sperm whale myoglobin or horseradish peroxidase, but qualitative results with the type 2 and 3 catalysts suggest that smaller observed rate constants will be found for the larger biological redox reagents. Further work is required to optimize the type 2 and 3 catalysts with respect to rate and to minimize problems with catalyst fouling by adsorption of biological materials. However, the results so far show that the high surface area catalysts prepared according to procedures summarized in Scheme III are effective in bringing about useful rates of reduction of biological redox reagents using H_2.

Experimental Section

Biological Materials. All heme proteins were the highest purity products obtained commercially from the Sigma Chemical Co. The needed materials were ordered on a "just-in-time" basis for delivery to ensure freshness and minimize storage. Horse heart cytochrome *c* (cyt *c* type VI), sperm whale myoglobin (Mb, type III), and horseradish peroxidase (POD, type VI) were stored in a darkened desiccator at −20 °C before use.

Procedures and Equipment. All active H_2 purges of the protein solutions were done through the space above the liquid level to guard against foaming and denaturing. Typically, the heme protein reduction experiments were conducted in a septum-sealed 1-cm path length quartz cuvette under 1 atm H_2. The catalyst (10 mg) was stirred in a 3.0-mL aqueous solution that contained the protein, 0.1 M $NaClO_4$ electrolyte, and 0.05 M NaH_2PO_4 buffer (pH 7.0). All the necessary manipulations of the protein solutions were done under the inert atmosphere. For example, a test tube containing the lyophilized POD, a second test tube containing 5 mL of the buffer solution, the cuvette containing the catalyst, and a magnetic stirring bar were each sealed off by a rubber septum and degassed with Ar for 15 min. The O_2-free POD solution was then prepared by transferring 4.0 mL of the buffer solution via syringe into the test tube containing POD. Finally, the starting reaction mixture for POD was prepared by transferring 3.0 mL of the protein solution via syringe to the cuvette with the catalyst. The reasons for undertaking such precaution to exclude O_2 are twofold. First, the exclusion of O_2 prevents the oxygenation reactions of the heme iron, leaving the desired reduction product, the ferro–heme active site of the reduced protein, in the pure "deoxy" form.[23] Second, removal of O_2 prevents the slow decomposition of the PQ^+ functionality formed in the activated viologen-based catalyst.[11]

The progress of the heme protein reductions was monitored by optical spectroscopy. The reaction mixture in the cuvette was centrifuged before the recording of each absorption spectrum (200–800 nm) on a Varian Cary 17 spectrophotometer. Typically, absorption spectra were recorded before and immediately after a short initial H_2 purge (~1 min). The time elapsed from the start of the initial H_2 purge to the completion of the recorded spectrum was generally 3–5 min. The majority of our heme protein reduction experiments were done after just the initial H_2 purge. The results are summarized in Table III. From the spectra collected for the reduction, the changes in solution composition and concentrations were determined with the aid of the molar absorptivity coefficients given in Table I. For those reductions that required more time beyond the initial run, the H_2 purge and the spectrum acquisition steps were repeated at longer reaction time. All spectra shown in the Figures 2–4 for cytochrome *c*, myoglobin, and peroxidase reductions agree completely with those found in the literature.[23] The reduction of cytochrome *c* and myoglobin with the millimolar concentrations required the dilution of a 0.03-mL sample from the reaction mixture to 3.0 mL so that the absorption spectra could be recorded within absorbance range of the Cary 17 spectrophotometer.

Acknowledgment. We thank the U.S. Department of Energy, Office of Basic Energy Sciences, Division of Chemical Sciences for support of this research.

Registry No. SiO_2, 7631-86-9; Pd, 7440-05-3; Pt, 7440-06-4; $PdCl_4^{2-}$, 14349-67-8; $PtCl_4^{2-}$, 13965-91-8; H_2, 1333-74-0; ferricytochrome *c*, 9007-43-6; peroxidase, 9003-99-0.

(22) Cammarata, V.; Crayston, J. A.; Wrighton, M. S., to be submitted.

(23) (a) Antonini, E.; Brunori, M. *Hemoglobin and Myoglobin in Their Reactions with Ligands*; North-Holland: Amsterdam, 1971; p 17. (b) Ochiai, E.-I. *Boinorganic Chemistry*; Allyn & Bacon: Boston, 1977; p 146. (c) Brune, D.; San Pietro, A. *Arch. Biochem. Biophys.* **1970**, *141*, 371. (d) Keilin, D.; Hartree, E. F. *Biochem. J.* **1951**, *49*, 88.